Journal of Applied Electrochemistry (2007) 37:21–26
DOI 10.1007/s10800-006-9224-x

Feasibility of using PtFe alloys as cathodes in direct methanol fuel cells

K. SCOTT, W. YUAN and H. CHENG*
School of Chemical Engineering & Advanced Materials, University of Newcastle upon Tyne, Newcastle upon Tyne, NE1 7RU, UK
*(*author for correspondence, fax:+44-0191-222-5292, e-mail: hua.cheng@ncl.ac.uk)*

Received 14 February 2006; accepted in revised form 24 April 2006

Key words: direct methanol fuel cell, Pt alloy catalysts, oxygen reduction, methanol crossover

Abstract

Carbon-supported platinum–iron catalysts were fabricated and characterised by means of scanning electron microscopy, energy-dispersive X-ray system and X-ray diffraction. The catalysts were tested in electrochemical half cells for oxygen reduction using voltammetry and steady-state polarisation measurements and in direct methanol fuel cells. Use of PtFe/C cathodes, instead of a Pt/C cathode, partially suppressed methanol oxidation and led to higher net oxygen reduction currents in the presence of methanol. Consequently, an increase in power density up to 30% was achieved in direct methanol fuel cells with PtFe/C cathodes, compared to that with Pt/C cathode. The influence of alloy composition and operation conditions on the cell performance has been investigated.

1. Introduction

The direct methanol fuel cell (DMFC) is attractive for portable and transportation applications due to its high energy density 2.25 kW h (kg methanol)$^{-1}$, high efficiencies of up to 40% and low operation temperatures (60–100 °C) [1, 2]. Current technology is based on polymer electrolyte membrane (PEM) cells. One of the challenges is to tackle the negative effect of methanol crossover from anode to cathode through the PEM, which decreases fuel efficiency and introduces parasitic currents due to methanol oxidation at Pt-based cathodes, overall resulting in a potential loss of up to 0.3–0.5 V [3–5].

Use of ruthenium chalcogenide catalysts, e.g. RuSeM (M = Mo, Re, Rh etc.) and RuSM (M = Rh, Re, Mo etc.), greatly suppresses methanol oxidation on these cathode catalysts, although their activity for the oxygen reduction reaction (ORR) is lower than for Pt catalysts [6–8]. Another approach is to use carbon-supported macrocycles and their derivatives of Fe or Co, e.g. iron tetramethoxyphenyl porphyrin, which show high methanol tolerance but their stability is a concern, especially under acidic conditions [9, 10]. The positive effect of alloying Pt with transition metals such as Cr, Fe, Co, Ni, etc. on methanol tolerance and stability of the Pt alloys has been demonstrated [3, 4], although the full potential of this type of catalyst has to be explored. In this study PtFe/C catalysts were fabricated and investigated for their electrochemical performance in half-cells and in direct methanol fuel cells.

2. Experimental

2.1. *Reagents, materials and apparatus*

The chemical reagents and materials with their respective suppliers are: H_2PtCl_6 (99.9%, Janssen), $Fe(NO_3)_3 \cdot 9H_2O$ (AnalaR, BDH), N_2H_4 (35 wt.% aqueous solution, Aldrich), H_2SO_4 (AnalaR, BDH), CH_3OH (99.99%, Fisher), carbon powder (Vulcan XC-72R, Cabot), carbon paper (TGPH120, E-TEK), PtRu/C (60 wt% Pt + Ru on Vulcan XC-72R, 1:1 in atomic ratio of Pt to Ru, E-TEK), PtFe/C (20 wt% Pt + Fe on Vulcan XC-72R, 1:1 in atomic ratio of Pt to Fe, E-TEK), Nafion® solution (5 wt%, Aldrich), Nafion® 117 membrane (DuPont), platinum mesh (20 cm^2, 99.99%, Goodfellow) and Hg/Hg_2SO_4 (saturated K_2SO_4) reference electrode (Russell). Deionised water (ELGASTAT B124 Water Purification Unit, the Elga group, England) and high purity gases (hydrogen, nitrogen, air and oxygen, BOC) were used.

2.2. *Preparation and characterisation of PtFe alloys*

The impregnation method was used to prepare carbon-supported PtFe alloy catalysts [11]. For example, 200 mg of Vulcan XC-72R carbon powder was dispersed in a

20 ml mixture of iso-propanol and deionised water (volume ratio 1:1) at 60 °C under magnetic stirring for 10 min. Then, 100 mg of H_2PtCl_6 was added dropwise and stirred for another 10 min. The same procedure was followed to add 94 mg $Fe(NO_3)_3 \cdot 9H_2O$. The solution pH was adjusted to 7 using 0.1 M N_2H_4 solutions and the final mixture was ultrasonicated for 30 min. The mixture was then filtered and alloyed at 750 °C for 1 h at a hydrogen flow rate of 100 ml min^{-1} before being annealed at 750 °C for 2 h at 100 ml N_2 min^{-1}. Three typical Pt:Fe catalysts were made with atomic ratios of 3.8:1, 1.2:1 and 1:2.7, which are referred to as 3.8Pt1Fe/C, 1.2Pt1Fe/C and 1Pt2.7Fe/C, respectively.

Scanning electron microscopy (SEM) and energy-dispersive X-ray (EDX) measurements were carried out using a JEOL JSM-5300LV scanning electron microscope with a ROUTEC UHV Dewar Detector at an acceleration voltage of 25 kV.

X-ray diffraction (XRD) analysis was performed with a Siemens D-5005 X-ray Diffractometer using Cu Kα radiation. The tube current was 100 mA and tube voltage was 40 kV. The 2θ angular regions between 20 and 100° were explored at a scan rate of 2 ° min^{-1}. The XRD pattern was compared to the International Centre for Diffraction Data® (ICDD®) [12]. The lattice parameters of the catalysts were calculated from broadening of the peak Pt (111) using the Scherrer equation [13]:

$$L = K\lambda / B\cos\theta \quad (1)$$

where L is the average length of the crystallite, B is the broadening of the line in units of 2θ and θ is Bragg diffraction angle, K is a constant approximately equal to 0.9 [4] and λ is wavelength. The relative intensity (i.e. average surface distribution) of the Pt (111) crystal face was calculated based on four main diffraction peaks, Pt (111), Pt (200), Pt (220) and Pt (311).

2.3. *Half-cell and fuel cell tests*

An undivided three-electrode glass cell (200 cm^3 in volume) was used for single electrode half-cell measurements. A loading of 1 mg Pt cm^{-2} was used for these gas diffusion electrodes, which were prepared by pasting a mixture of the catalyst + Nafion® (0.3 mg cm^{-2}) + iso-propanol onto carbon paper and then hot-pressing at 100 kg cm^{-2} and 130 °C. During measurements, nitrogen or oxygen gas (25 $cm^3 min^{-1}$) passed through the electrode and penetrated into solution. Cyclic voltammetry and steady-state galvanostatic polarisation were performed using a 10A-20V Ministat Potentiostat (Sycopel Scientific Limited, England) with a PCI-100 signal generator (Sycopel Scientific Limited, England).

All membrane electrode assemblies (MEAs) were fabricated under comparable conditions, e.g. using the same catalyst loading, 1 mg Pt cm^{-2} + 0.52 mg Ru cm^{-2} for anodes and 1.0 mg Pt cm^{-2} for cathodes. Details of the MEA fabrication and the DMFC operation are described elsewhere [14].

3. Results and discussion

3.1. *Structural characteristics*

Figure 1 shows SEM for the 1.2Pt1Fe/C material. The catalyst surface appears highly porous consisting of cauliflower-like clusters. The chemical compositions of three PtFe/C catalysts determined by EDX are shown in Table 1. Different Pt:Fe ratios were obtained by controlling amounts of Pt and Fe salts during the preparation (Table 1). Figure 2 compares XRD pictures for the PtFe/C and Pt/C materials. The main diffraction peaks observed in the spectra can be identified as the crystal faces Pt (111), Pt (200), Pt (220) and Pt (311) with slightly changed 2θ positions (Figure 2 and Table 1), which is evidence of the formation of PtFe alloys [15]. The lattice parameter decreased and the relative intensity of the Pt (111) crystal face increased with increasing Fe content (Table 1). All three samples exhibited only a face-centred cubic structure with the lattice parameters of 0.3815–0.3835 nm, which are smaller than that of the Pt/C, i.e. 0.3928 nm, suggesting that the crystal axis was shortened due to the presence of Fe.

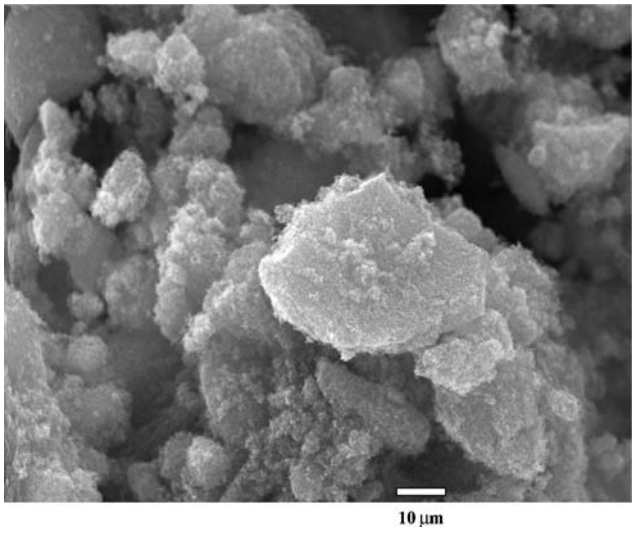

Fig. 1. Scanning electron micrograph of the 1.2Pt1Fe/C material (× 1000).

Table 1. EDX and XRD data of the PtFe/C catalysts

Sample	EDX data (atomic, %)			XRD data		
	C	Pt	Fe	$2\theta^a$/°	L^b/nm	$I_{111}/\Sigma I_{hkl}$/%
1Pt2.7Fe	89.43	2.86	7.71	40.08	0.3815	59.1
1.2Pt1Fe	95.75	2.35	1.91	39.97	0.3828	58.7
3.8Pt1Fe	95.28	3.74	0.98	39.91	0.3825	58.2
Pt				39.81	0.3928	55.2

[a] Pt (111) crystal face.
[b] The lattice parameters, which were calculated using (111) crystal face of Pt.

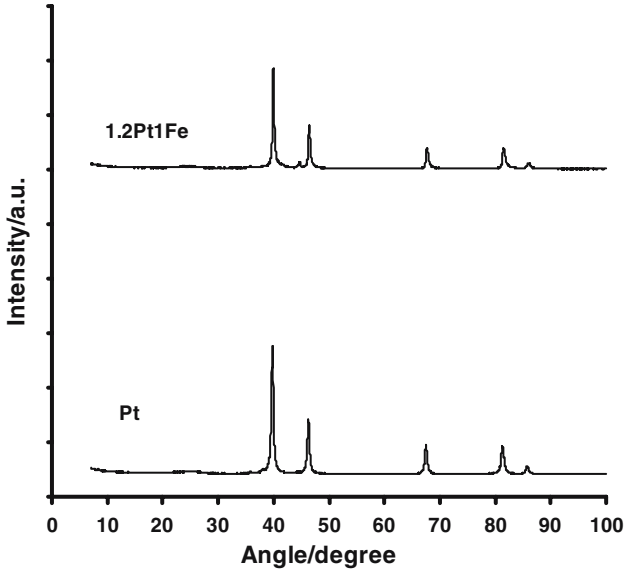

Fig. 2. Powder XRD patterns of the Pt/C and the 1.2Pt1Fe/C materials.

3.2. *Test of PtFe/C catalysts in half-cells*

Figure 3 compares the performance of the 1Pt2.7Fe/C and the Pt/C gas diffusion electrodes in 0.5 M sulphuric acid + 1 M methanol solution, where current density is normalised to the Pt loading. Methanol was oxidised on both electrodes, which resulted in two peaks with current densities of 32.2 and 6.9 mA cm^{-2} for the Pt/C and 1Pt2.7Fe/C electrode, respectively, suggesting higher methanol tolerance of the latter. Current densities for the ORR in 1 M methanol solution was higher at the 1Pt2.7Fe/C than at the Pt/C. Similar behaviour was observed during the reverse scan. These observations mean that alloying Pt with Fe could alleviate the negative effect of methanol oxidation on the ORR.

Figure 4 and Table 2 show steady-state polarisation data obtained at –0.4 V using the Pt/C and PtFe/C electrodes, in O_2 –saturated 0.5 M H_2SO_4 solutions, with and without methanol. Reduction currents increased rapidly to yield a well-defined flat plateau for the two electrodes within several seconds. The addition of methanol led to decreased current densities. All the PtFe/C catalysts showed better performance than the Pt/C as indicated by the higher current densities at fixed potential, e.g. 81.2 and 65.0 mA cm^{-2} at – 0.4 V, for the 1.2Pt1Fe/C and the Pt/C electrodes (Table 2), respectively.

As is well-known, iron alone does not form active sites for ORR, but alloying it with Pt can lead to performance enhancement due to several effects, such as a structural effect (higher relative content of the Pt(111) crystal face and lattice contractions [1, 4], an electronic effect (more 5d vacancies and enhanced O_2 adsorption [16] and chemical effects (higher peroxide decomposition activity [4]. Better methanol tolerance of the PtFe alloys than of Pt can be attributed to the role of Fe addition. On the other hand, iron itself is not active for methanol oxidation and its addition will partly block contact between Pt particles and methanol molecules, which suppresses methanol oxidation on the binary-component catalyst. Quantum calculations show that the strong reactivity of Pt with organic compounds is depressed by alloying with Fe [17], resulting in higher methanol tolerance of PtFe cathodes, compared to Pt.

3.3. *Test of PtFe/C cathodes in direct methanol fuel cells*

3.3.1. *Influence of alloy composition*

DMFCs with the 1.2Pt1Fe/C cathode showed better performance than that with the Pt/C cathode, e.g. an increase of 10% in power density (curves a and b,

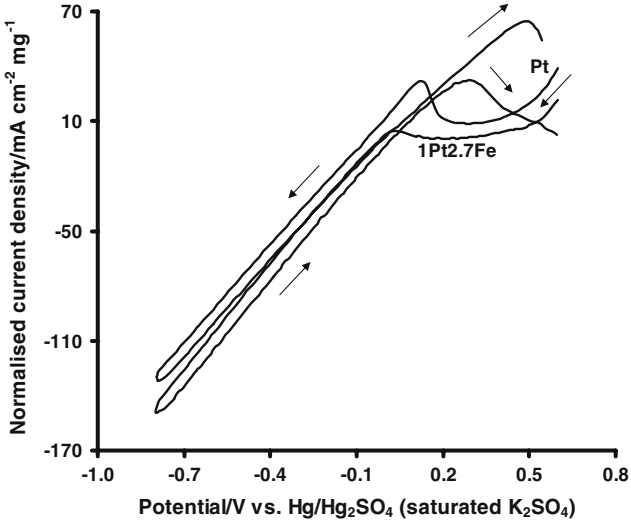

Fig. 3. Cyclic voltammograms on the 1Pt2.7Fe/C and Pt/C gas diffusion electrodes in 1 M CH_3OH + 0.5 M H_2SO_4 solution saturated with O_2 (25 cm^3 min^{-1}). Undivided glass cell. Counter electrode: Pt mesh (20 cm^2). Scan rate: 50 mV s^{-1}. Temperature: 18 ± 0.5 °C. The arrows indicate the scan directions.

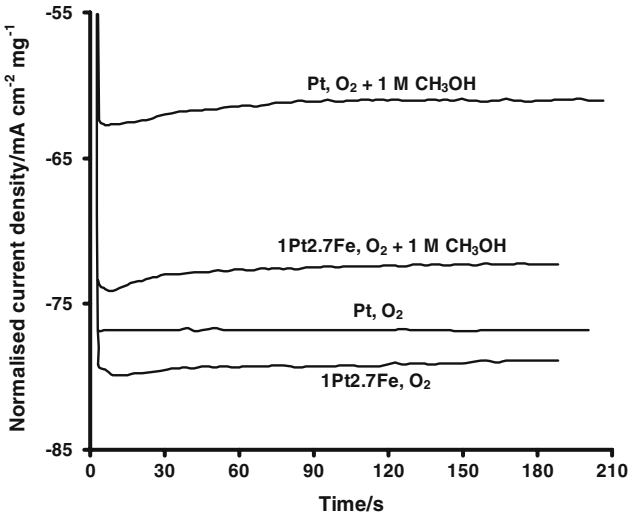

Fig. 4. Potentiostatic curves on the 1.2Pt1Fe/C and Pt/C gas diffusion electrodes in O_2 – saturated 0.5 M H_2SO_4 solution with or without 1 MCH_3OH. Pt loading: 1 mg Pt cm^{-2}. Controlled potential: –0.4 V vs. Hg/Hg_2SO_4 (saturated K_2SO_4). Other conditions as in Figure 3.

Table 2. Net current densities obtained from the half-cell tests[a]

Cathode	Methanol concentration/M			
	0	0.1	0.5	1.0
Pt	76.8	65.0	62.4	60.2
3.8Pt1Fe	80.3	75.5	67.3	65.2
1.2Pt1Fe	81.2	76.8	68.5	66.4
1Pt2.7Fe	82.9	78.6	70.2	68.1

[a] Net current density was obtained by subtracting the current density measured in the N_2-saturated solution from that in the O_2-saturated solution. Conditions as in Figure 4.

Figure 5), which may be contributed to the enhanced activity for ORR and better methanol tolerance of the PtFe/C cathodes, as mentioned previously. The alloy catalysts showed better performance (ca. 20 mV) than commercial catalyst from E-TEK (curves d and e, Figure 5).

3.3.2. *Influence of fuel and oxidant conditions*

Table 3 and Figure 6 show the effects of increasing methanol concentration and temperature on MEAs with the PtFe/C and Pt/C cathodes. Decreases of 106 and 130 mV in OCV and 14.5 and 21.3 mW cm^{-2} in peak power density were observed for the 1.2Pt1Fe/C and Pt/C cathodes, respectively. These data highlight the beneficial effect of operating the DMFC with a PtFe/C catalyst. A further improvement in methanol tolerance of PtFe alloys is required because the performance decreased with increasing methanol concentration (curves a and c, Figure 6). As expected, the performance was enhanced by increasing temperature (curves a and b, Figure 6) due to improved electrode kinetics.

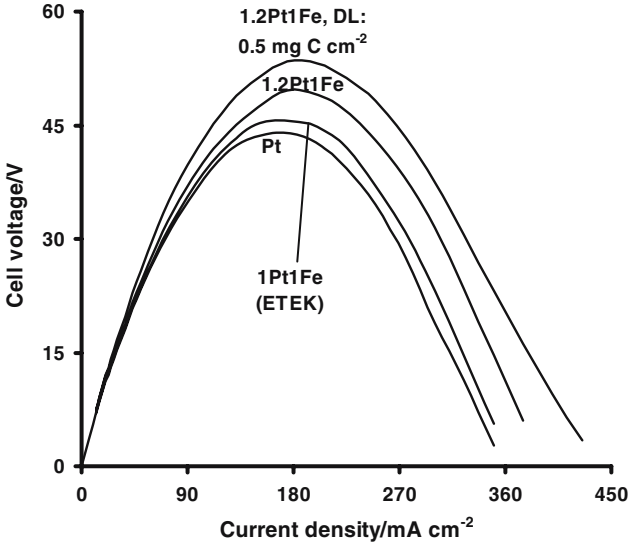

Fig. 5. Steady-state power density vs. current density curves for the fuel cells with the 1.2Pt1Fe/C, 1Pt1Fe/C (E-TEK) and Pt/C cathodes. Active area of the cell: 4 cm^2. Anode: PtRu/C (1.52 mg PtRu cm^{-2}). Cathode loading: 1.0 mg Pt cm^{-2}. Membrane: Nafion® 117. Carbon loading of diffusion layer: 0.5 or 1 mg C cm^{-2}. Fuel: 1 M CH_3OH (10 cm^3 min^{-1}). Oxidant: O_2 (ambient pressure, 200 cm^3 min^{-1}). Temperature: 90 °C.

Table 3. Data obtained from the DMFC tests with 1, 2 and 4 M methanol fuels[a]

Cathodes	OCV/V	P_{Peak}/mW cm^{-2}	$j_{maximum}$/mA cm^{-2}
1.2Pt1Fe (1 M)	0.708	49.5	390
1.2Pt1Fe (2 M)	0.685	46.4	380
1.2Pt1Fe (4 M)	0.602	35.0	335
Pt (1 M)	0.692	43.9	350
Pt (2 M)	0.665	33.2	325
Pt (4 M)	0.562	22.6	230

[a] Other conditions as in Figure 5.

Cell performance under different oxidant conditions is shown in Figure 7. Operating the cell with O_2 rather than air, provided better performance due to enhanced oxidant supply. An increase in oxidant pressure provided higher concentration driving force and improved the DMFC performance, e.g. raising the pressure to 1 bar O_2 led to an increase in peak power density from 48.7 to 68.5 mW cm^{-2} (curves a and b, Figure 7), due to improved oxygen reduction kinetics. Under high pressures, lower oxidant flow rates, e.g. <0.001 LPM, could be used.

3.3.3. *Influence of diffusion layers*

The effect of gas diffusion layer (GDL, carbon paper + carbon powder) was investigated and Figure 5 shows an example. Treatment of GDL at 300 °C improved performance and a further improvement was achieved by reducing the carbon loading from 1 to 0.5 mg C cm^{-2} (curves c and d, Figure 5). It is reasonably expected that the treatment removes impurities present in the non-treated GDL and results in improved surface pores and, hence, greater reactant permeability and superior water management. An additional effect of using the GDL with 0.5 rather than 1 mg C cm^{-2} was the lower ohmic losses, e.g. a reduction of 200 kΩ in cell

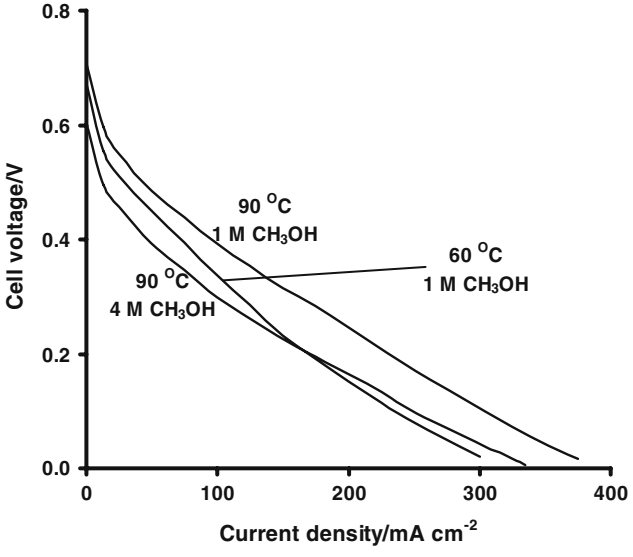

Fig. 6. Effects of fuel conditions on the DMFC performance. Fuel: 1 or 4 M CH_3OH (10 cm^3 min^{-1}). Temperature: 60 or 90 °C. Other conditions as in Figure 5.

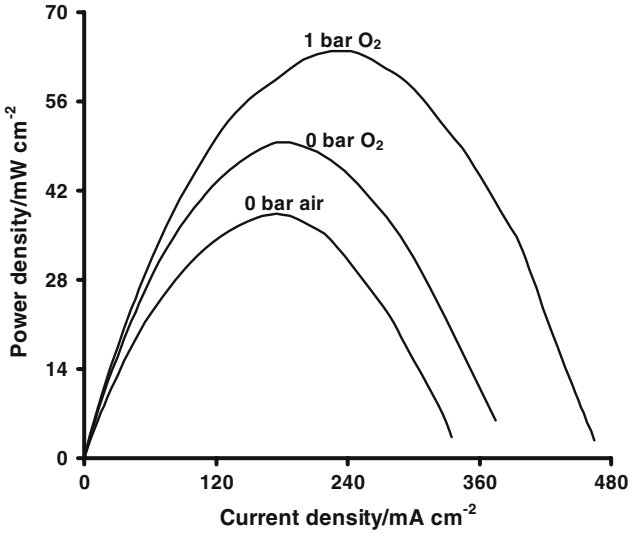

Fig. 7. Effects of oxidant conditions on the DMFC performance. Oxidant: 0 or 1 bar O_2 or 0 bar air. Other conditions as in Figure 5.

resistance at 10 cm^3 min^{-1} H_2O and ambient temperature was observed.

3.3.4. *Durability test*

The stability of the PtFe/C catalysts was tested and compared to that of Pt; data are shown in Figure 8. There was fluctuation in the cell voltage when a fresh solution was added or operation restarted after an interruption. Before the durability test, the MEAs were used for over 300 h for conditioning, measurements and maintenance. The MEAs with the alloy cathodes displayed less deterioration than that with the Pt cathode, e.g. about 30 and 110 mV decrease in cell voltage for the alloy and Pt cathodes after a period of 100 h, respectively. The better stability of the PtFe alloys can be partially attributed to the contraction of Pt–Pt distance occurring in the PtFe alloys (Table 1), which led to stronger combination between the Pt particles. Formation of very strong O–Fe bonds also changed the segregation profile of the PtFe alloy surface, resulting in a more stable configuration [18]. As is well-known, Fe has a strong tendency to alloy with carbon, which increases stability of PtFe/C systems. A slight decrease in performance was due to chemical and thermal deactivation during operation.

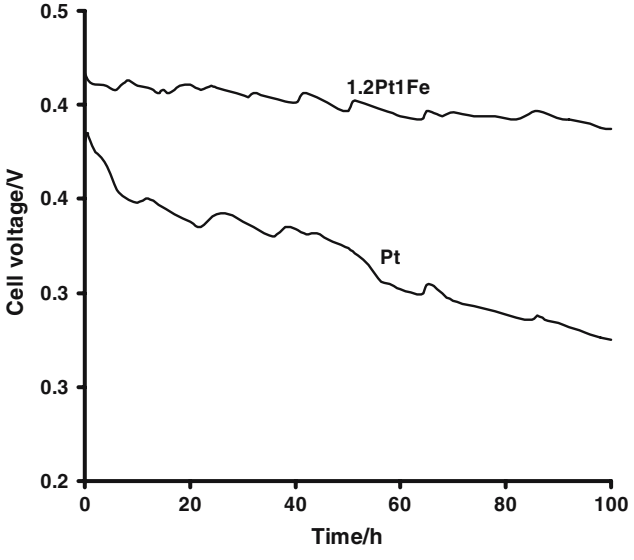

Fig. 8. Cell voltage change with time for the DMFCs with the 1.2Pt1Fe/C and Pt/C cathodes at 50 mA cm^{-2} and 60 °C. Other conditions as in Figure 5.

4. Conclusions

Alloying of Pt with Fe suppressed methanol oxidation on PtFe cathodes, leading to higher activity and better stability, compared to Pt alone, e.g. higher net reduction current density in half-cells and higher power density in DMFCs. All alloys showed better performance than the E-TEK PtFe sample. Increasing cell temperature increased power density owing to the enhanced reaction kinetics. The DMFC performance decreased with increasing methanol concentration, suggesting that the PtFe alloys are not completely tolerant to the presence of methanol. The performance was improved by operating the DMFC with O_2 rather than air and increasing pressure led to higher power densities due to the enhanced oxidant supply. Better gas permeability could be achieved by treated thin GDL at 300 °C.

Acknowledgements

The authors thank the Carbon Trust and EPSRC for funding. The work was performed in research facilities provided through an EPSRC/HEFCE Joint Infrastructure Fund award (No. JIF4NESCEQ).

References

1. W.H. Lizcano-Valbuena, V.A. Paganin, C.A.P. Leite, F. Galembeck and E.R. Gonzalez, *Electrochim. Acta* **48** (2003) 3869.
2. X. Ren, P. Zelenay, S. Thomas, J. Davey and S. Gottesfeld, *J. Power Sources* **86** (2000) 111.
3. H. Yang, N. Alonso-Vante, C. Lamy and D.L. Akins, *J. Electrochem. Soc.* **152** (2005) A704.
4. W. Li, W. Zhou, H. Li, Z. Zhou, B. Zhou, G. Sun and Q. Xin, *Electrochim. Acta* **49** (2004) 1045.
5. A.S. Arico, S. Srinivasan and V. Antonucci, *Fuel Cells* **1** (2001) 133.
6. M. Bron, P. Bogdanoff, S. Fiechter, I. Dorbant, M. Hilgendorff, H. Schulenburg and H. Tributsch, *J. Electroanal. Chem.* **500** (2001) 510.
7. R.W. Reeve, P.A. Christensen, A.J. Dickinson, A. Hamnett and K. Scott, *Electrochim. Acta* **45** (2000) 4237.
8. T.J. Schmidt, U.A. Paulus, H.A. Gasteiger, N. Alonso-Vante and R.J. Behm, *J. Electrochem. Soc.* **147** (2000) 2620.
9. P. Convert, C. Coutanceau, F. Claguen and C. Lamy, *J. Appl. Electrochem.* **31** (2001) 945.
10. M. Lefevre and J.P. Dodelet, *Electrochim. Acta* **48** (2003) 2749.

11. Z. Wei, H. Guo and Z. Tang, *J. Power Sources* **62** (1996) 233.
12. http://www.icdd.com (the reference codes are 06–0696 for Fe and 04–0802 for Pt).
13. R.L. Snyder, *in* E. Lifshin (ed.), *X-ray Characterization of Materials*, (Weinheim, Wiley-VCH, 1999), pp. 1–103.
14. H. Cheng and K. Scott, *J. Power Sources* **123** (2003) 137.
15. J.T. Hwang and J.S. Chung, *Electrochim. Acta* **38** (1993) 2715.
16. R. Hirsch, F. Delbecq, P. Sautet and J. Hafner, *J. Power Sources* **217** (2003) 354.
17. A. Fortunelli and A.M. Velasco, *J. Mol. Struct.: THEOCHEM* **586** (2002) 17.
18. G.Q. Sun, J.T. Wang and R.F. Savinell, *J. Appl. Electrochem.* **28** (1998) 1087.